

1  
2 **Resonant pumping of  $d-d$  crystal field electronic transitions as a mechanism**  
3 **of ultrafast optical control of the exchange interactions in iron oxides**

4 R. V. Mikhaylovskiy<sup>1,2a</sup>, T. J. Huisman<sup>1</sup>, V. A. Gavrichkov<sup>3</sup>, S. I. Polukeev<sup>3</sup>, S. G. Ovchinnikov<sup>3</sup>,  
5 D. Afanasiev<sup>1,4</sup>, R. V. Pisarev<sup>5</sup>, Th. Rasing<sup>1</sup>, and A. V. Kimel<sup>1</sup>

6 <sup>1</sup>*Radboud University, Institute for Molecules and Materials, Heyendaalseweg 135, 6525 AJ*  
7 *Nijmegen, the Netherlands*

8 <sup>2</sup>*Department of Physics, Lancaster University, Bailrigg, Lancaster LA1 4YW, United Kingdom*

9 <sup>3</sup>*Kirensky Institute of Physics, Federal Research Center KSC SB RAS, 660036 Krasnoyarsk, Russia*

10 <sup>4</sup>*Kavli Institute of Nanoscience, Delft University of Technology, P.O. Box 5046, 2600 GA Delft, the*  
11 *Netherlands*

12 <sup>5</sup>*Ioffe Physical-Technical Institute, Russian Academy of Sciences, 194021 St. Petersburg, Russia*  
13

14 The microscopic origin of ultrafast modification of the ratio between the symmetric ( $J$ ) and  
15 antisymmetric ( $D$ ) exchange interaction in antiferromagnetic iron oxides is revealed, using  
16 femtosecond laser excitation as a pump and terahertz emission spectroscopy as a probe. By tuning the  
17 photon energy of the laser pump pulse we show that the effect of light on the  $D/J$  ratio in two  
18 archetypical iron oxides  $\text{FeBO}_3$  and  $\text{ErFeO}_3$  is maximized when the photon energy is in resonance with  
19 a spin and parity forbidden  $d-d$  transition between the crystal-field split states of  $\text{Fe}^{3+}$  ions. The  
20 experimental findings are supported by a multi-electron model, which accounts for the resonant  
21 absorption of photons by  $\text{Fe}^{3+}$  ions. Our results reveal the importance of the parity and spin-change  
22 forbidden, and therefore often underestimated,  $d-d$  transitions in ultrafast optical control of magnetism.  
23  
24

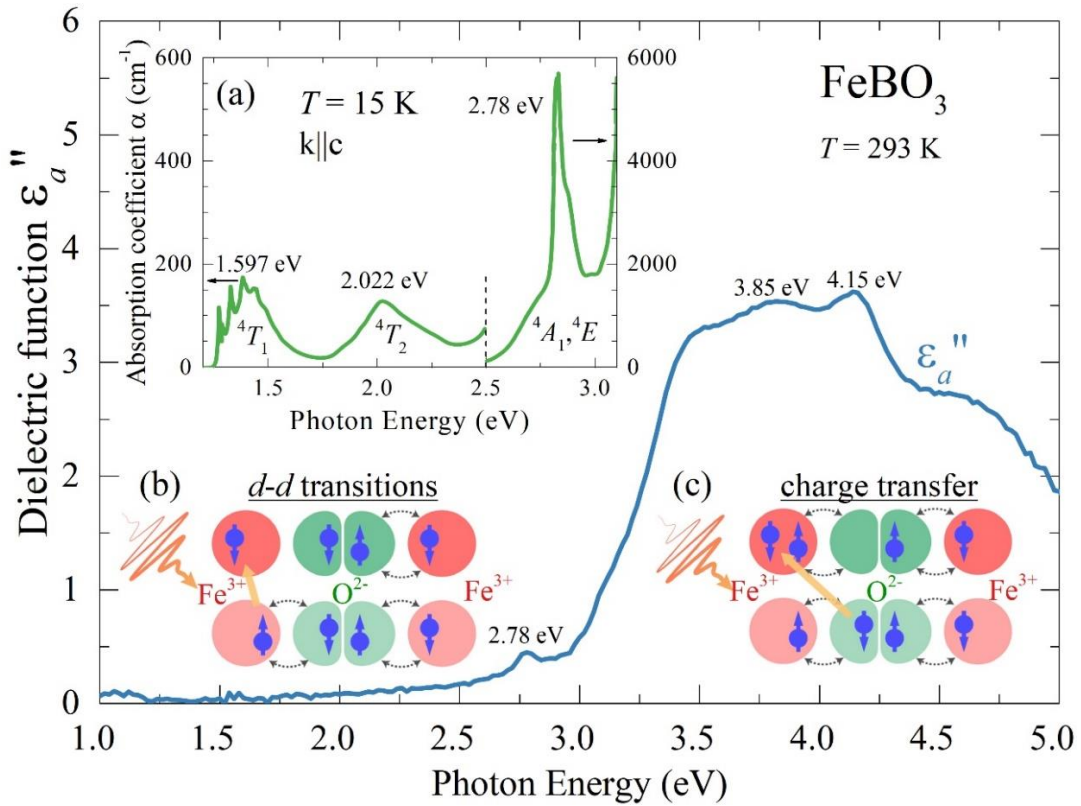
---

<sup>a</sup> Email for correspondence: [r.mikhaylovskiy@lancaster.ac.uk](mailto:r.mikhaylovskiy@lancaster.ac.uk)

25 The short-range spin-spin exchange interaction that results in long-range magnetic order is one of the  
26 important demonstrations of the quantum nature of matter. Remarkably, the strength of the exchange  
27 interaction in magnetically ordered materials expressed in terms of effective magnetic fields can reach  
28 1000 Tesla in which the spin precession period is typically shorter than a picosecond. Controlling the  
29 exchange interaction by sub-picosecond laser pulses is thus a very appealing approach to search for a  
30 new scenario of the fastest possible control of magnetism [1].

31 The symmetric part of the exchange energy  $W_{\text{ex}}$  between two magnetic sublattices  $\mathbf{S}_1$  and  $\mathbf{S}_2$   
32  $W_{\text{ex}} = J\mathbf{S}_1\mathbf{S}_2$  is responsible for the very existence of long-range magnetic order. During recent years,  
33 the modulation of the symmetric exchange interaction by femtosecond laser pulses has been a subject  
34 of experimental and theoretical studies [2-19]. Its antisymmetric counterpart, the relativistic  
35 Dzyaloshinskii-Moriya energy  $W_D = \mathbf{D}\times[\mathbf{S}_1\times\mathbf{S}_2]$ , contributes to the emergence of weak  
36 ferromagnetism [20], multiferroicity [21] and magnetic skyrmions [22]. The possibility of ultrafast  
37 optical control of the ratio between  $J$  and  $D$  has been reported for various transition metal oxides and  
38 motivated several theoretical proposals to manipulate magnetic textures through optical control [23-  
39 28]. However, presently available theoretical models fail to describe the change of exchange in realistic  
40 materials, hence there is no information which optical transitions one must pump to change  $D/J$   
41 efficiently. In this Letter we experimentally reveal that the weak, and thus often overlooked,  $d-d$   
42 transitions are responsible for the efficient modification of the  $D/J$  exchange ratio. We also suggest a  
43 multi-orbital theory that can explain the effect.

44 To observe the optical modification of  $J$  and/or  $D$ , one can use the fact that in a broad class of  
45 antiferromagnetic iron oxides (iron borate  $\text{FeBO}_3$ , hematite  $\alpha\text{-Fe}_2\text{O}_3$ , and orthoferrites  $R\text{FeO}_3$ , with  $R$   
46 being a rare-earth element) the ratio  $D/J$  defines the canting angle of the two magnetic sublattices of  
47  $\text{Fe}^{3+}$  ions. Therefore, in these materials an ultrafast change of the exchange constants  $J$  and/or  $D$  results  
48 in coherent spin motion that can be reliably separated from the heat-driven and other incoherent  
49 dynamics. Particularly, perturbation of  $J$  and/or  $D$  triggers the quasi-antiferromagnetic (q-AFM) mode  
50 of antiferromagnetic resonance [29] involving periodic oscillation of the canting angle at a THz  
51 frequency. The spin motion acts as *ac* magnetic dipole emitting coherent THz electro-magnetic waves,  
52 which were measured experimentally. The excitation of the antiferromagnetic resonance by light can  
53 be seen as an impulsive stimulated Raman process, known as inverse magnetic refraction.  
54 Microscopically, this effect involves the change of the  $J/D$  ratio [29].

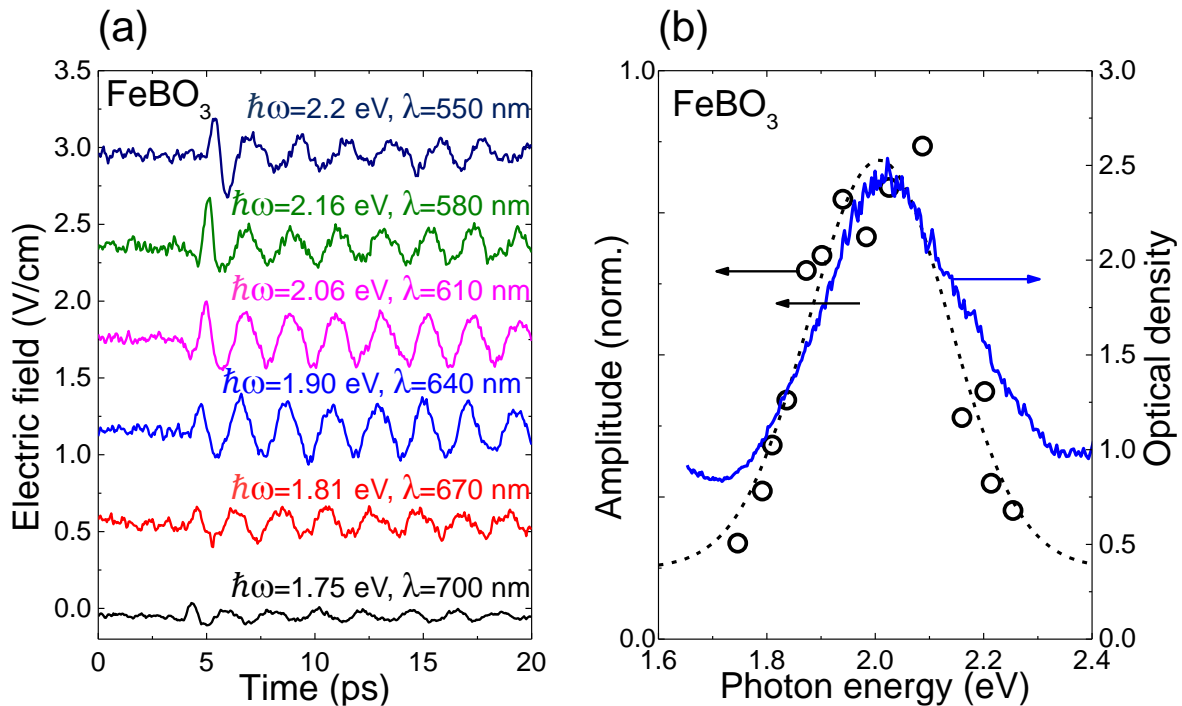


55

56 Fig. 1. (Color online). Main panel: The imaginary part of the  $\text{FeBO}_3$  dielectric function as a  
 57 function of photon energy measured using a spectroscopic ellipsometer. The response is  
 58 dominated by strong charge transfer transitions above 3 eV. Insets: (a). Absorption coefficient of  
 59 antiferromagnetic iron oxide  $\text{FeBO}_3$ . Absorption was measured for light propagating along the  
 60 optical axis. Absorption bands due to the  $d-d$  transitions from the  ${}^6A_1$  ground state to the  ${}^4T_1$ ,  ${}^4T_2$ ,  
 61  ${}^4A_1$ ,  ${}^4E$  excited states are indicated. (b). Modulation of the superexchange interaction due to the  
 62 pumping of the  $d-d$  transitions involving a spin flip from  $S = 5/2$  in the ground state to  $S = 3/2$  in  
 63 the excited states. (c). Schematics showing the modulation of the superexchange interaction by a  
 64 laser induced charge transfer.

65 The optical absorption of the iron oxides is defined by charge-transfer *electric dipole* transitions  
 66 between the oxygen  $p$  orbitals and the  $d$  orbitals of the  $\text{Fe}^{3+}$  ions and  $d-d$  transitions of the single  $\text{Fe}^{3+}$   
 67 ion (see Fig. 1 and Refs. 30-32). The virtual hopping of the electrons between  $\text{Fe}^{3+}$  and  $\text{O}^{2-}$  ions gives  
 68 rise to superexchange interaction resulting in the antiferromagnetic ordering ( $J > 0$ ). Therefore, it is  
 69 natural to assume that the laser pulse excites the charge-transfer transitions, thereby modifying the  
 70 hopping and consequently the exchange coupling between the neighboring  $\text{Fe}^{3+}$  ions. This scenario is  
 71 illustrated in Fig. 1c and has been discussed earlier for manganites [33] and  
 72 ferromagnetic/antiferromagnetic heterostructures [34,35].

73 The weak and broad  $d-d$  absorption bands arise due to the inter-orbital transitions between the  $3d$ -  
 74 states split by the crystal field (see Fig. 1 for  $\text{FeBO}_3$  and Refs. 30,31 for other iron oxides). These  
 75 transitions are forbidden in the electric-dipole approximation. However, they become partially allowed  
 76 due to mixing of  $p-d$  atomic states of opposite parity by phonons and/or due to the inversion symmetry  
 77 breaking at the position of the magnetic ion. Moreover, these electronic excitations between the  $3d^5$   
 78 states of the  $\text{Fe}^{3+}$  ion require a spin-change from  $S = 5/2$  to  $S = 3/2$  that is also forbidden for optical  
 79 transitions in the electric-dipole approximation. However, this restriction is removed by accounting  
 80 for the spin-orbit coupling. A femtosecond optical pulse can excite these transitions resonantly and  
 81 drive electrons into a new orbital configuration with a different spin value, thereby perturbing the  
 82 superexchange (Fig. 1b). Even though most pump-probe experiments use pump pulses with a photon  
 83 energy of 1.55 eV very close to the  $d-d$  absorption bands in iron oxides, the inter-orbital transitions in  
 84 magnetic cations in ultrafast light-spin interactions has so far got very limited attention [36-38] and  
 85 their role in the control of the  $D/J$  exchange ratio still remains unclear.



86

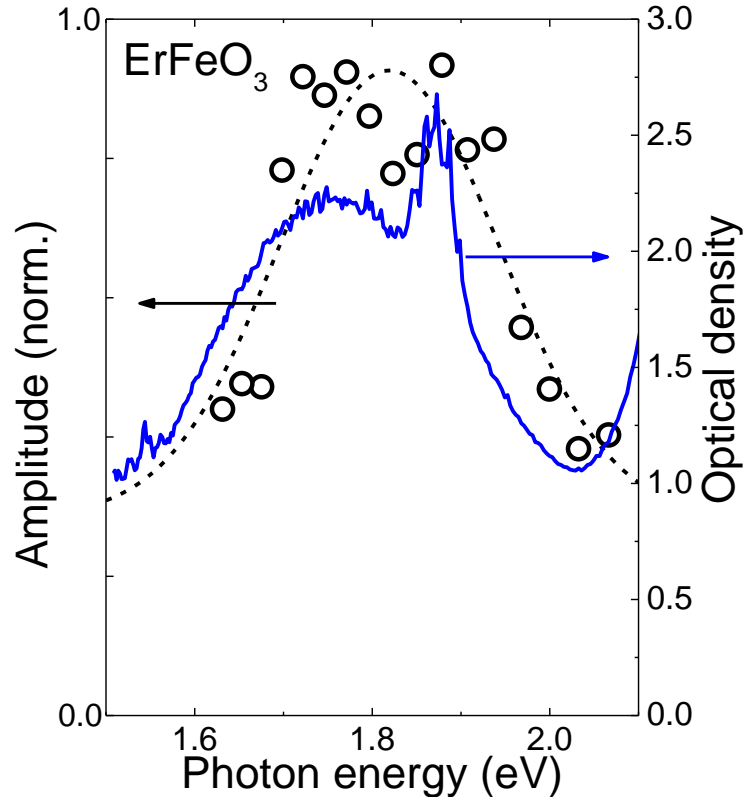
87 Fig. 2. (Color online). (a). Waveforms of the THz electric field emitted from  $\text{FeBO}_3$  excited by  
 88 femtosecond pulses of different photon energy (wavelength). The slight change in the signal delay  
 89 is due to the inequality of the optical paths for different wavelengths. (b). Amplitude of the THz  
 90 waveforms as a function of the pump photon energy (open circles) shown together with the  
 91 measured optical density of the same sample (solid line). The amplitude is normalized with  
 92 respect to the pump power, which varied for different wavelengths. Dashed line is a guide to the  
 93 eye.

94 Spectral measurements with wavelength-tuneable laser pulses can provide an efficient way for  
95 unveiling the microscopic mechanisms responsible for the modification of the exchange interaction.  
96 To establish a spectroscopic correlation between the observed effects and the absorption bands, we  
97 employed THz emission spectroscopy [39], with tuneable photon energy of the pump laser pulse [40].  
98 The measured THz signal is directly related to the magnetization dynamics by linear Maxwell  
99 equations [41]. The samples were brought into a single domain state by an in-plane bias magnetic field  
100 of  $\sim 0.1$  Tesla.

101 Initially we studied a rhombohedral calcite-type single crystal of iron borate  $\text{FeBO}_3$ . The  $370 \mu\text{m}$  thick  
102 sample was cut perpendicularly to the  $z$ -axis, i.e. with the antiferromagnetic vector and weak  
103 ferromagnetic moment in the basal  $xy$ -plane. Fig 2a shows the time traces of the electric field emitted  
104 from the photo-excited sample for different pump pulse photon energies. In order to maximize the  
105 detected signal, the measurements were done at the low temperature of 10 K. As one can see, the  
106 signals consist of quasi-monochromatic oscillations at a frequency of about 450 GHz, matching the  
107 frequency of the q-AFM mode of  $\text{FeBO}_3$ . The observed waveforms do not depend neither on the  
108 polarization of the pump light, nor on the crystal orientation, while their sign does change when  
109 changing the polarity of the applied magnetic field. The signals have all the properties attesting the  
110 excitation of the q-AFM by modulation of the superexchange interaction [29]. By fitting the  
111 experimental data with decaying sinusoidal functions we retrieved the amplitude of the q-AFM mode,  
112 which is plotted in Fig. 2b as a function of the pump photon energy. The amplitude shows a clear  
113 resonant behavior in the vicinity of the  ${}^6A_1 \rightarrow {}^4T_2$  transition, with a central energy at  $\sim 2$  eV (see Fig.  
114 1a). To further support this observation, we measured the optical transmission as a function of photon  
115 energy for this particular sample. The resulting optical density perfectly matches the dependence of  
116 the q-AFM amplitude (see Fig. 2b), confirming that the optical excitation of the q-AFM mode and  
117 hence the modulation of the  $D/J$  exchange ratio is due to the resonant pumping of the  ${}^6A_1 \rightarrow {}^4T_2$   
118 transition.

119 To test whether the observed resonant behavior is present in other iron oxides, we repeated similar  
120 THz emission measurements on  $\text{ErFeO}_3$ , belonging to the orthorhombic crystal family of rare-earth  
121 orthoferrites. In this material we also observed THz emission corresponding to the q-AFM mode [29].  
122 As an example, Fig. 3 shows the photon energy dependence of the amplitude of the q-AFM mode of  
123 the  $\text{ErFeO}_3$  sample. The optical density of the sample is also shown in Fig. 3. Very similar to  $\text{FeBO}_3$   
124 the amplitude peaks at the photon energy corresponding to the  ${}^6A_1 \rightarrow {}^4T_2$  absorption band. At the same

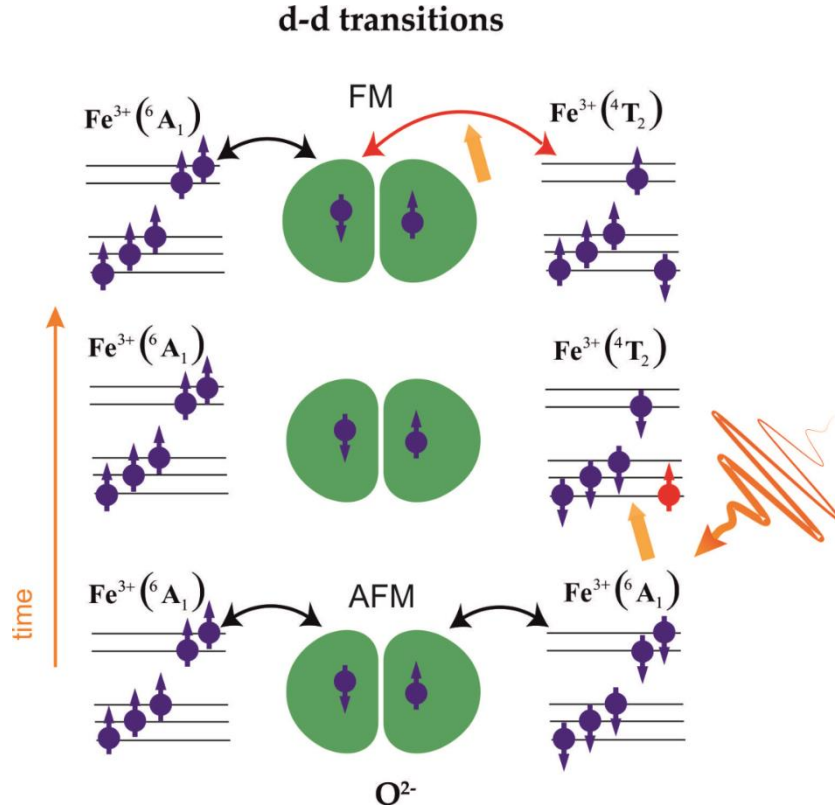
125 time, there is no clear evidence for contribution of  $f-f$  transitions between  $\text{Er}^{3+}$  localized states (seen as  
 126 narrow peaks just below 1.9 eV in Fig. 3) to the perturbation of the  $D/J$  ratio. However, THz emission  
 127 efficiency seems to be centered at a slightly higher photon energy compared to the  $d-d$  absorption  
 128 band. It may indicate some influence of the  $f-f$  transitions or it may also be due to the velocity mismatch  
 129 between THz and optical waves at the different frequencies.



130  
 131 Fig. 3. (Color online). Amplitude of the THz waveforms as a function of the pump photon energy  
 132 (open circles) shown along with the measured optical density of the  $\text{ErFeO}_3$  sample (solid line).  
 133 The amplitude is normalized as in Fig. 2. Dashed line is a guide to the eye. The narrow feature at  
 134  $\sim 1.87$  eV is due to  $f-f$  transitions in  $\text{Er}^{3+}$  ions. This measurement was performed at room  
 135 temperature.

136 Using a  $\beta$ -barium borate (BBO) single crystal the photon energy of the fundamental laser pulse at 1.55  
 137 eV was doubled to 3.1 eV in order to pump the samples in the region of the strong absorption close to  
 138 their charge-transfer gap (Fig. 1). However, we observed no THz emission from all samples in this  
 139 case. Although this result stands against a charge-transfer based mechanism of the superexchange  
 140 modulation (Fig. 1c), one has to bear in mind that due to the strong absorption of more than  $10^3 \text{ cm}^{-1}$   
 141 at 3.1 eV, the penetration depth of the laser pulse is only  $\sim 1 \mu\text{m}$ , which is much less than that in the  
 142 transparency region ( $\sim 70 \mu\text{m}$ ). Therefore, the THz signal is emitted from a significantly thinner part

143 of the sample than in the 1.7-2.3 eV range. Most probably it falls below the noise level and thus requires  
 144 more detailed study. Nonetheless, we can confidently state that the pumping of  $d-d$  transitions  
 145 positioned below the charge transfer transitions dominates in the optical modulation of the  $D/J$



146 exchange ratio in the iron oxides.

147 Fig.4. (Color online). Illustration of the photoinduced modulation of the superexchange interaction  
 148 in an iron oxide. In the ground state (lower panel) the hopping results in the antiferromagnetic  
 149 alignment of spins. The optical excitation flips one spin in an iron ion (red one, middle panel) and  
 150 as a result in the excited state (upper panel) the interaction becomes ferromagnetic and more spins  
 151 change their orientation.

152 The existing models for non-equilibrium exchange [1] neglect the possibility of laser-induced spin  
 153 flips due to magnetic dipole transitions or non-local optical transitions associated with the generation  
 154 of exciton-magnon pairs at the neighboring lattice sites [42]. Here we theoretically discuss how the  
 155 incorporation of the excited states of the magnetic cation can result in a change of the superexchange  
 156 interaction under optical pumping. We employ the formalism recently developed in Ref. 43. We  
 157 consider a rare-earth free case of  $\text{FeBO}_3$ . In its ground state a non-zero value of the spin canting angle  
 158  $\varphi_0 \approx 0.95^\circ$  is observed, which can be explained as a result of Dzyaloshinskii-Moriya interaction [44].

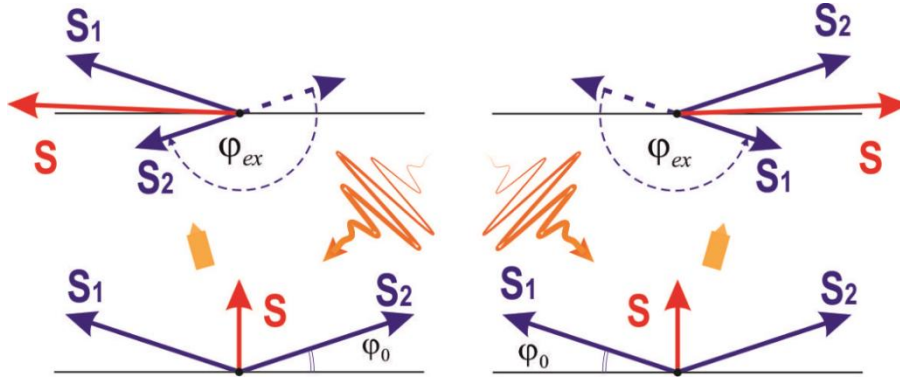
159 Under optical pumping, the  ${}^4T_2$  triplet excited states with spin  $S = \frac{3}{2}$  are populated. The conclusion  
160 of the multi-electron approach [43] is that the resonant occupation of some excited states of the  $\text{Fe}^{3+}$   
161 ions under optical pumping may change the value and even the sign of the superexchange interaction  
162 between the excited ion and a neighboring ion in the ground state. For the  ${}^4T_2$  excited term of the  $\text{Fe}^{3+}$   
163 ion a ferromagnetic (FM) type of exchange has been found [45].

164 To clarify the physics of the complicated multielectron approach [43] we illustrate the optical  
165 modulation of the superexchange interaction in Fig. 4. At equilibrium the superexchange arises from  
166 electron hopping between two  $\text{Fe}^{3+}$  ions in the ground state with  $S=5/2$  via an  $\text{O}^{2-}$  ion (see the lower  
167 part of Fig.4). One spin-up ( $\uparrow$ ) electron from the left cation virtually hops to oxygen forming a  $\uparrow\downarrow$  pair  
168 and back with the same spin projection. Another oxygen spin-up electron also virtually hops to the  
169 right cation to the spin-down ( $\downarrow$ ) electron and back. Such mechanism favours the antiferromagnetic  
170 (AFM) ordering between the neighboring  $\text{Fe}^{3+}$  ions. After a photoinduced  $d-d$  transition (upper part of  
171 Fig. 4) one of the electrons in the excited ion is antiparallel to the others and the spin of the excited  
172 term becomes  $3/2$ . The virtual hopping of the spin-up electron from the left cation in the ground state  
173 to oxygen and back is the same as it was before the laser excitation, while for the right excited cation  
174 the virtual hopping of the second oxygen spin-down electron and back is possible for the spin-up  
175 cation, where four electrons of the excited  ${}^4T_2$  term remain parallel to the spin of the left cation, so  
176 their interaction becomes ferromagnetic (FM). We should remark that this picture is just a cartoon of  
177 the complicated calculation [43,46] where the effective spin Hamiltonian including both ions in the  
178 ground and excited states is obtained by means of a perturbation theory.

179 Besides the qualitative picture shown in Fig.4, direct calculations [43] lead to an AFM superexchange  
180 in the ground state, and to a FM interaction  $J_{ij}^{\text{ex}}$  for  $\text{Fe}^{3+}$  ions under optical pumping at A and B  
181 absorption lines of a set of A ( ${}^4T_1$ ), B ( ${}^4T_2$ ) and C ( ${}^4A_1, {}^4E$ ) optical  $d-d$  excitations [45]. The optically  
182 induced FM contributions to the superexchange  $J_{ij}^{\text{ex}}$  dominate due to the largest overlap of  $2p$  oxygen  
183 orbitals with excited  $\text{Fe}^{3+} ({}^4T_2)$  ions. When excited in the C line, the FM contribution of the interaction  
184  $J_{ij}^{\text{ex}}$  vanishes due to a sharp drop in the overlapping for the excited  $\text{Fe}^{3+} ({}^4A_1, {}^4E)$  ions. The AFM state  
185 of  $\text{FeBO}_3$  is maintained at equilibrium at a low concentration of excited ion pairs  $\text{Fe}^{3+} ({}^4T_2)$ -



186  $\text{Fe}^{3+} (^6A_1)$  with FM exchange. We assume that the optical transition occurs instantaneously, and the  
 187 lifetime of the excited  $\text{Fe}^{3+}$  ion exceeds the characteristic time of the change in the superexchange



188 interaction  $h/W \sim 10^{-15}$  s, where  $W$  is the band width.

189

190 Fig.5 (Color online). Change of the relative orientation of the magnetic moments in an  
 191 exchange-coupled pair of  $\text{Fe}^{3+}$  ions due to the sign change of the superexchange interaction from  
 192 AFM ( $J_{ij}^{ex} < 0$ , lower part) to FM ( $J_{ij}^{ex} > 0$ , upper part) induced by the laser pulse. The lower  
 193 part shows the relative orientation of the spin moments  $\mathbf{S}_1$  and  $\mathbf{S}_2$  of the two ions in the ground  
 194 state. The upper part shows the relative orientation of  $\mathbf{S}_1$  and  $\mathbf{S}_2$  of the two ions in which one is  
 195 in the excited state. Left part of the figure corresponds to optical  $d-d$  transitions in the magnetic  
 196 sublattice A, where  $S_1 = 5/2$ ,  $S_2 = 3/2$  and the right part corresponds to  $d-d$  transitions in the  
 197 sublattice B, where  $S_1 = 3/2$ ,  $S_2 = 5/2$ .

198

199 The spin-orbit interaction appears already in the first order of perturbation theory and results in a small  
 200 change in the spin-canting angle. However, this last contribution is not important in the model under  
 201 discussion, because the main effect is the rearrangement of spins of the two AFM sublattices shown in  
 202 Fig. 5. The lower part of Fig. 5 shows four spins in the ground state, two  $\mathbf{S}_1$  from the A sublattice and  
 203 two  $\mathbf{S}_2$  from the B sublattice. The excitation of the A sublattice ion is shown in the left part and that of  
 204 the B ion in the right part. There are two major effects of the  $d-d$  excitations that should be taken into  
 205 account. The first one is the spin change from  $S=5/2$  to  $S=3/2$ , shown by dotted lines in the upper part  
 206 of Fig. 5. The second effect is the excited spin rotation with the total spin  $\mathbf{S}$  oriented left or right  
 207 depending on which cation has been excited. It is evident that both sublattices are excited similarly, so  
 208 the total magnetization is not changed. Nevertheless, the localized  $d-d$  excitation forms the excited  
 209 total magnetic moment  $\mathbf{S}$ . Therefore, the spin canting angle  $\varphi_{ex}$  at the optically excited  $\text{Fe}^{3+} (^4T_2)$  state  
 210 is modified as determined by the changed values of the superexchange and spin-orbit interactions:

211

$$\varphi_{ex} = \left( \pi - \frac{D_{ex}}{J_{ij}^{ex}} \right). \quad (1)$$

212

213

214

215

216

217

218

219

220

221

222

223

224

225

226

227

228

229

230

231

232

### Acknowledgements

233

234

235

236

These processes are illustrated in Fig. 5. The phase shift  $\sim \pi$  arises due to a spin flip at the optically excited  $\text{Fe}^{3+} (^4T_2)$  center in one of the magnetic sublattices under the action of the optically-induced FM  $J_{ij}^{ex} > 0$  superexchange interaction.

The most remarkable result of the optical response in  $\text{FeBO}_3$  under resonant pumping of the  ${}^6A_1 \leftrightarrow {}^4T_2$  transition is the sign change in the superexchange interaction from AFM  $J_{ij} < 0$  to FM  $J_{ij}^{ex} > 0$ . Because the optical absorption in both sublattices of the AFM material is identical, the total magnetic moment under optical pumping is still close to zero and no macroscopic FM ordering arises (Fig. 5). Evidently, in the linear regime the concentration  $x$  of optically excited centers is proportional to the intensity of the optical pump, which should not be too large to avoid dielectric breakdown. Using the absorption coefficient of  $\text{FeBO}_3$  (Fig. 1), the size of its unit cell [47], the pump fluence and the excitation volume, we may estimate that in our experiment  $x \leq 10^{-3}$ . This number is in line with our estimation of the modulation of the ratio  $D/J \geq 10^{-4}$  [29].

In summary, we have shown that optical control of the exchange interaction in iron oxides can be achieved by resonant excitation of the  $d-d$  crystal field transitions in magnetic  $\text{Fe}^{3+}$  ions, involving a spin change  $\Delta S=1$ . Our finding demonstrates another alternative to the currently used theoretical approaches based on the Hubbard model for the description of ultrafast light-spin interactions. It reveals novel opportunities for resonant optical control of the exchange interaction and thus opens up new perspectives for experimental and theoretical research in the field of ultrafast magnetism.

We thank A. Toonen and S. Semin for technical assistance. The work at Radboud University was supported by de Nederlandse Organisatie voor Wetenschappelijk Onderzoek (NWO) and the European Research Council ERC Grant agreement No. 339813 (Exchange). R.V.M. thanks ERC, Grant agreement No 852050 (MAGSHAKE). V.A.G., S.I.P. and S.G.O. are thankful to the Russian Science

237 Foundation for the financial support under the grant 18-12-00022. The theoretical part of this research  
238 was performed by V.A.G., S.I.P. and S.G.O. under the RSF grant 18-12-00022. The contribution of  
239 R.V.P. into the experimental part was supported by the RSF grant 16-12-10456.

240

1. J. H. Mentink. Manipulating magnetism by ultrafast control of the exchange interaction. *J. Phys.: Cond. Mat.* **29**, 453001 (2017).
2. H.-S. Rhie, H. Dürr and W. Eberhardt. Femtosecond electron and spin dynamics in Ni/W(110) films. *Phys. Rev. Lett.* **90**, 247201 (2003).
3. A. Melnikov, I. Radu, U. Bovensiepen, O. Krupin, K. Starke, E. Matthias and M. Wolf. Coherent optical phonons and parametrically coupled magnons induced by femtosecond laser excitation of the Gd (0001) surface. *Phys. Rev. Lett.* **91**, 227403 (2003).
4. J. Wang, I. Cotoros, K. Dani, X. Liu, J. Furdyna and D. Chemla. Ultrafast enhancement of ferromagnetism via photoexcited holes in GaMnAs. *Phys. Rev. Lett.* **98**, 217401 (2007).
5. S. Wall, D. Prabhakaran, A. T. Boothroyd, and A. Cavalleri. Ultrafast coupling between light, coherent lattice vibrations, and the magnetic structure of semicovalent LaMnO<sub>3</sub>. *Phys. Rev. Lett.* **103**, 097402 (2009).
6. M. Först, et al. Driving magnetic order in a manganite by ultrafast lattice excitation. *Phys. Rev. B* **84**, 241104 (2011).
7. R. Carley, et al. Femtosecond laser excitation drives ferromagnetic gadolinium out of magnetic equilibrium. *Phys. Rev. Lett.* **109**, 057401 (2012).
8. T. Li, et al. Femtosecond switching of magnetism via strongly correlated spin–charge quantum excitations. *Nature* **496**, 69 (2013).
9. R. R. Subkhangulov, et al. All-optical manipulation and probing of the d-f exchange interaction in EuTe. *Sci. Rep.* **4**, 4368 (2014).
10. J. H. Mentink and M. Eckstein. Ultrafast quenching of the exchange interaction in a Mott insulator. *Phys. Rev. Lett.* **113**, 057201 (2014).
11. M. Matsubara, et al. Ultrafast optical tuning of ferromagnetism via the carrier density. *Nat. Comm.* **6**, 6724 (2015).
12. J. H. Mentink, K. Balzer and M. Eckstein. Ultrafast and reversible control of the exchange interaction in Mott insulators. *Nat. Comm.* **6**, 6708 (2015).
13. B. Frietsch, et al. Disparate ultrafast dynamics of itinerant and localized magnetic moments in gadolinium metal. *Nat. Comm.* **6**, 8262 (2015).
14. J. O. Johansson, J.-W. Kim, E. Allwright, D. M. Rogers, N. Robertson and J.-Y. Bigot. Directly probing spin dynamics in a molecular magnet with femtosecond time-resolution. *Chem. Sci.* **7**, 7061 (2016).
15. S. Eich et al. Band structure evolution during the ultrafast ferromagnetic-paramagnetic phase transition in cobalt. *Sci. Adv.* **3**, e1602094 (2017)
16. Ph. Tengdin, et al. Critical behavior within 20 fs drives the out-of-equilibrium laser-induced magnetic phase transition in nickel. *Sci. Adv.* **4**, eaap9744 (2018).
17. S. F. Maehrlein, et al. Dissecting spin-phonon equilibration in ferrimagnetic insulators by ultrafast lattice excitation. *Science Advances* **4**, eaar5164 (2018).
18. D. Afanasiev, et al. Ultrafast spin dynamics in photodoped spin-orbit Mott insulator Sr<sub>2</sub>IrO<sub>4</sub>. *Phys. Rev. X* **9**, 021020 (2019).

19. A. Ron, et al. Ultrafast enhancement of ferromagnetic spin exchange induced by ligand-to-metal charge transfer. arXiv:1910.06376 (2019).
20. I. Dzyaloshinsky. A thermodynamic theory of “weak” ferromagnetism of antiferromagnetics. *J. Phys. Chem. Solids* **4**, 241 (1958).
21. I. A. Sergienko and E. Dagotto. Role of the Dzyaloshinskii-Moriya interaction in multiferroic perovskites. *Phys. Rev. B* **73**, 094434 (2006).
22. U. K. Röbler, A. N. Bogdanov and C. Pfleiderer. Spontaneous skyrmion ground states in magnetic metals. *Nature* **442**, 797 (2006).
23. C. Dutreix, E. A. Stepanov, and M. I. Katsnelson. Laser-induced topological transitions in phosphorene with inversion symmetry. *Phys. Rev. B* **93**, 241404(R) (2016).
24. E. A. Stepanov, C. Dutreix, and M. I. Katsnelson. Dynamical and reversible control of topological spin textures. *Phys. Rev. Lett.* **118**, 157201 (2017).
25. H. Fujita and M. Sato. Ultrafast generation of skyrmionic defects with vortex beams: Printing laser profiles on magnets. *Phys. Rev. B* **95**, 054421 (2017).
26. D. Yudin, D. R. Gulevich, and M. Titov. Light-induced anisotropic skyrmion and stripe phases in a Rashba ferromagnet. *Phys. Rev. Lett.* **119**, 147202 (2017).
27. T. H. Kim, P. Grünberg, S. H. Han, and B. K. Cho. Precessional switching of antiferromagnets by electric field induced Dzyaloshinskii-Moriya torque. *Phys. Rev. B* **97**, 184427 (2018).
28. F. Freimuth, S. Blügel, and Y. Mokrousov. Spin-orbit torques and tunable Dzyaloshinskii-Moriya interaction in Co/Cu/Co trilayers. *Phys. Rev. B* **98**, 024419 (2018).
29. R. V. Mikhaylovskiy, et al. Ultrafast optical modification of exchange interactions in iron oxides. *Nat. Comm.* **6**, 8190 (2015).
30. D. L. Wood, J. P. Remeika, and E. D. Kolb. Optical spectra of rare-earth orthoferrites. *J. Appl. Phys.* **41**, 5315 (1970).
31. A. M. Kalashnikova, V. V. Pavlov, R. V. Pisarev, L. N. Bezmaternykh, M. Bayer, Th. Rasing. Linear and nonlinear optical spectroscopy of gadolinium iron borate  $\text{GdFe}_3(\text{BO}_3)_4$ . *JETP Letters* **80**, 293 (2004)
32. R. V. Pisarev, A. S. Moskvina, A. M. Kalashnikova, and Th. Rasing. Charge transfer transitions in multiferroic  $\text{BiFeO}_3$  and related ferrite insulators. *Phys. Rev. B* **79**, 235128 (2009).
33. H. B. Zhao, et al. Coherent spin precession via photoinduced antiferromagnetic interactions in  $\text{La}_{0.67}\text{Ca}_{0.33}\text{MnO}_3$ . *Phys. Rev. Lett.* **107**, 207205 (2011).
34. X. Ma, et al. Ultrafast spin exchange-coupling torque via photo-excited charge-transfer processes. *Nat. Comm.* **6**, 8800 (2015).
35. Z. Zheng, et al. Ultrafast modulation of exchange-coupling induced anisotropy in Fe/CoO by laser induced charge transfer. *Appl. Phys. Lett.* **110**, 172401 (2017).
36. R. Iida, et al. Spectral dependence of photoinduced spin precession in  $\text{DyFeO}_3$ . *Phys. Rev. B* **84**, 064402 (2011).
37. D. Talbayev, et al. Spin-dependent polaron formation dynamics in  $\text{Eu}_{0.75}\text{Y}_{0.25}\text{MnO}_3$  probed by femtosecond pump-probe spectroscopy. *Phys. Rev. B* **91**, 064420 (2015).
38. Y. M. Sheu, Y. M. Chang, C. P. Chang, Y. H. Li, K. R. Babu, G. Y. Guo, T. Kurumaji, and Y. Tokura. Picosecond creation of switchable optomagnets from a polar antiferromagnet with giant photoinduced Kerr rotations. *Phys. Rev. X* **9**, 031038 (2019).

39. G. Gallot and Grischkowsky. Electro-optic detection of terahertz radiation. *J. Opt. Soc. Am. B* **16**, 1204 (1999).
40. R. V. Mikhaylovskiy, et al. Terahertz magnetization dynamics induced by femtosecond resonant pumping of  $\text{Dy}^{3+}$  subsystem in the multisublattice antiferromagnet  $\text{DyFeO}_3$ . *Phys. Rev. B* **92**, 094437 (2015).
41. T. J. Huisman, R. V. Mikhaylovskiy, A. Tsukamoto, Th. Rasing, A. V. Kimel. Simultaneous measurements of terahertz emission and magneto-optical Kerr effect for resolving ultrafast laser-induced demagnetization dynamics. *Phys. Rev. B* **92**, 104419 (2015).
42. V. V. Eremenko, N.F. Kharchenko, Y.G. Litvinenko, V.M. Naumenko, in book: *Magneto-Optics and Spectroscopy of Antiferromagnets*, Springer-Verlag New York, X, 276 p., 1992.
43. V. A. Gavrichkov, S. I. Polukeev, and S. G. Ovchinnikov. Contribution from optically excited many-electron states to the superexchange interaction in Mott-Hubbard insulators. *Phys. Rev. B* **95**, 144424 (2017).
44. S. G. Ovchinnikov and V V Rudenko. Anisotropic interactions in magnetic crystals with S-state ions. *Nanostructures. Physics-USpekhi*, **57**, 1180 (2014).
45. See Supplementary file.
46. V. A. Gavrichkov, S. I. Polukeev, and S. G. Ovchinnikov. Cation spin and superexchange interaction in oxide materials below and above spin crossover under high pressure. *Phys. Rev. B* **101**, 094409 (2020).
47. R.Diehl. Crystal structure refinement of ferric borate,  $\text{FeBO}_3$ . *Solid State Communications* **17**, 743 (1975).